

## CONDENSED MATTER PHYSICS

Discovery of slow magnetic fluctuations and critical slowing down in the pseudogap phase of  $\text{YBa}_2\text{Cu}_3\text{O}_y$ Jian Zhang,<sup>1</sup> Zhaofeng Ding,<sup>1</sup> Cheng Tan,<sup>1</sup> Kevin Huang,<sup>1\*</sup> Oscar O. Bernal,<sup>2</sup> Pei-Chun Ho,<sup>3</sup> Gerald D. Morris,<sup>4</sup> Adrian D. Hillier,<sup>5</sup> Pabitra K. Biswas,<sup>5</sup> Stephen P. Cottrell,<sup>5</sup> Hui Xiang,<sup>6</sup> Xin Yao,<sup>6,7</sup> Douglas E. MacLaughlin,<sup>8</sup> Lei Shu<sup>1,7†</sup>

The origin of the pseudogap region below a temperature  $T^*$  is at the heart of the mysteries of cuprate high-temperature superconductors. Unusual properties of the pseudogap phase, such as broken time-reversal and inversion symmetry are observed in several symmetry-sensitive experiments: polarized neutron diffraction, optical birefringence, dichroic angle-resolved photoemission spectroscopy, second harmonic generation, and polar Kerr effect. These properties suggest that the pseudogap region is a genuine thermodynamic phase and are predicted by theories invoking ordered loop currents or other forms of intra-unit-cell (IUC) magnetic order. However, muon spin rotation ( $\mu\text{SR}$ ) and nuclear magnetic resonance (NMR) experiments do not see the static local fields expected for magnetic order, leaving room for skepticism. The magnetic resonance probes have much longer time scales, however, over which local fields could be averaged by fluctuations. The observable effect of the fluctuations in magnetic resonance is then dynamic relaxation. We have measured dynamic muon spin relaxation rates in single crystals of  $\text{YBa}_2\text{Cu}_3\text{O}_y$  ( $6.72 < y < 6.95$ ) and have discovered “slow” fluctuating magnetic fields with magnitudes and fluctuation rates of the expected orders of magnitude that set in consistently at temperatures  $T_{\text{mag}} \approx T^*$ . The absence of any static field (to which  $\mu\text{SR}$  would be linearly sensitive) is consistent with the finite correlation length from neutron diffraction. Equally important, these fluctuations exhibit the critical slowing down at  $T_{\text{mag}}$  expected near a time-reversal symmetry breaking transition. Our results explain the absence of static magnetism and provide support for the existence of IUC magnetic order in the pseudogap phase.

## INTRODUCTION

The mysterious pseudogap phase in high-temperature superconducting cuprates has been the subject of an enormous amount of research (1–4) but with little consensus on either its origin or its role in high-temperature superconductivity. The name arises from the loss of low-lying electronic excitations below a temperature  $T^*$ , which depends strongly on the hole concentration on  $\text{CuO}_2$  planes. This loss results in considerable modification of properties connected with these excitations, but their nature has been difficult to determine. Even whether or not  $T^*$  is in fact a phase transition temperature has been controversial.

Recent experiments have shown that, consistent with a phase transition, time-reversal symmetry (5, 6) and spatial rotation and inversion symmetries (7–9) are broken below  $T^*$  in a number of cuprate superconductors. However, lattice translational symmetry is preserved, indicating that the antiferromagnetism that lies near the pseudogap phase in the temperature-doping phase diagram is not involved. The unbroken translational symmetry has focused attention on the phenomena within the crystalline unit cell. In particular, the broken time-reversal symmetry is predicted by theories that invoke states with intra-unit-cell (IUC) magnetic order (10–12). However, doubt has been cast on the existence of IUC magnetic order: Local static magnetic fields of the expected

magnitude were not observed in muon spin rotation ( $\mu\text{SR}$ ) (13–18) or nuclear magnetic resonance (NMR) (19, 20) experiments.  $\mu\text{SR}$  and NMR are magnetic resonance techniques in which spin probes (implanted muons or nuclei) are sensitive to magnetic behavior on the local (atomic) scale.  $\mu\text{SR}$  in particular is capable of detecting nearby static magnetic moments in the range of 0.001 to 0.01  $\mu_B$  and did not do so in cuprate systems where neutron diffraction measurements observed moments of the order of 0.1  $\mu_B$ .

IUC magnetic order would be retained, and the absent static field would be accounted for, if the ordered moments fluctuate among alternate orientations (15, 18, 19). This would average the local field  $B_{\text{loc}}(t)$  at spin-probe sites to zero for time scales longer than a characteristic correlation time  $\tau_c$ . These fluctuations could be due to finite-size domains of an ordered phase with different field orientations (21), as seen in tunneling spectroscopy (22). For NMR and  $\mu\text{SR}$ , the experimental time scale for this averaging is considerably longer ( $\gtrsim 10^{-5}$  s) than that for the other techniques ( $\lesssim 10^{-10}$  s). Thus, all experiments would be consistent if the fluctuations were “slow,” with  $\tau_c$  between these limits.

Averaging or “motional narrowing” of  $B_{\text{loc}}(t)$  (the term comes from the effect of nuclear motion on static NMR line broadening in an applied field) occurs in the rapid fluctuation limit  $\gamma B_{\text{loc}}^{\text{rms}} \tau_c \ll 1$ , where  $\gamma$  is the gyromagnetic ratio of the nucleus or muon and  $B_{\text{loc}}^{\text{rms}} = \langle B_{\text{loc}}^2(t) \rangle^{1/2}$  is the root-mean-square (rms) local field. For the muon,  $\gamma = \gamma_\mu = 8.5156 \times 10^8 \text{ s}^{-1} \text{ T}^{-1}$ . The IUC-ordered moments per triangular plaquette obtained from neutron diffraction [0.05 to 0.1  $\mu_B$  in  $\text{YBa}_2\text{Cu}_3\text{O}_{6.66}$  (5, 6) and progressively lower at higher  $y$ ] give dipolar field values  $B_{\text{loc}} = 1$  to 10 mT at candidate muon sites in the unit cell of  $\text{La}_{2-x}\text{Sr}_x\text{CuO}_4$  (15). For these fields, the above inequality is satisfied for  $\tau_c \lesssim 10^{-6}$  s, which is in the range of experimental consistency. Thus,  $B_{\text{loc}}(t)$  gives rise to dynamic or “spin-lattice” nuclear or muon spin relaxation. Itoh *et al.* (23) have reported “ultraslow” fluctuations in  $\text{HgBa}_2\text{CaCu}_2\text{O}_{6+\delta}$  that may be of this kind.

In  $\mu\text{SR}$  experiments, the motionally narrowed dynamic muon spin relaxation rate in zero applied field (ZF) is given by  $\lambda_{\text{ZF}} = (\gamma_\mu B_{\text{loc}}^{\text{rms}})^2 \tau_c$

<sup>1</sup>State Key Laboratory of Surface Physics, Department of Physics, Fudan University, Shanghai 200433, People's Republic of China. <sup>2</sup>Department of Physics and Astronomy, California State University, Los Angeles, CA 90032, USA. <sup>3</sup>Department of Physics, California State University, Fresno, CA 93740, USA. <sup>4</sup>TRIUMF, Vancouver, British Columbia V6T 2A3, Canada. <sup>5</sup>ISIS Facility, Science and Technology Facilities Council Rutherford Appleton Laboratory, Harwell Science and Innovation Campus, Chilton, Didcot OX11 0QX, UK. <sup>6</sup>State Key Lab for Metal Matrix Composites, Key Laboratory of Artificial Structures and Quantum Control (Ministry of Education), Department of Physics and Astronomy, Shanghai Jiao Tong University, Shanghai 200240, People's Republic of China. <sup>7</sup>Collaborative Innovation Center of Advanced Microstructures, Nanjing 210093, People's Republic of China. <sup>8</sup>Department of Physics and Astronomy, University of California, Riverside, Riverside, CA 92521, USA.

\*Present address: National High Magnetic Field Laboratory, Tallahassee, FL 32310, USA.

†Corresponding author. Email: leishu@fudan.edu.cn

(24, 25). The relaxation rate measured in a longitudinal magnetic field (LF) (that is, the magnetic field parallel to the initial muon polarization) depends on the magnitude  $H_L$  of the field, an effect of sweeping the muon Zeeman frequency through the fluctuation noise power spectrum (24, 25). For Markovian fluctuations with a single well-defined correlation time  $\tau_c$ , the LF relaxation rate  $\lambda_{LF}$  in a field  $H_L$  is given by the so-called Redfield relation (24)

$$\lambda_{LF}(H_L) = \frac{\gamma_\mu^2 (B_{loc}^{rms})^2 \tau_c}{1 + (\gamma_\mu H_L \tau_c)^2} \quad (1)$$

The dependence of  $\lambda_{LF}$  on  $H_L$ , if observed to be of the form of Eq. 1, provides estimates of  $\tau_c$  and  $B_{loc}^{rms}$ . More generally, one expects a decrease of  $\lambda_{LF}$  for  $\gamma_\mu H_L$  greater than a characteristic fluctuation rate  $1/\tau_c$ , in which case  $\tau_c$  and  $B_{loc}^{rms}$  from fits of Eq. 1 to the data are heuristic estimates of the characteristic time and field scales. The Redfield relation has been widely applied in  $\mu$ SR to characterize dynamic fluctuating magnetic fields in strongly correlated electron systems, for example, in the heavy fermion superconductor  $\text{PrOs}_4\text{Sb}_{12}$  (26).

Here, we report the discovery of slow magnetic fluctuations in single crystals of  $\text{YBa}_2\text{Cu}_3\text{O}_y$ ,  $y = 6.72, 6.77, 6.83$ , and  $6.95$  (superconducting transition temperatures  $T_c = 72, 80, 88$ , and  $91$  K, respectively) via the field dependence of the  $\mu$ SR dynamic relaxation. Consistency with Eq. 1 is found, and values of  $\tau_c$  and  $B_{loc}^{rms}$  are obtained. We also find maxima at  $T_{mag} \approx T^*$  in the temperature dependences of the rates in ZF and LF. This is consistent with critical slowing down of magnetic fluctuations near the transition and demonstrates that these fluctuations are associated with the IUC order. There is considerable statistical uncertainty because the measured relaxation rates are near the limit of the technique, but standard statistical analysis techniques (see below) demonstrate the validity of our conclusions.

## RESULTS

We performed LF- $\mu$ SR experiments on samples with  $y = 6.72, 6.77$ , and  $6.83$ . The field dependence of the exponential relaxation rate  $\lambda_{LF}$  was measured for these samples at temperatures below  $T^*$  and above  $T_c$  for  $2 \text{ mT} \leq \mu_0 H_L \leq 400 \text{ mT}$ . The minimum field was chosen to be much larger than the  $\sim 0.1$ -mT quasi-static field from nuclear dipoles (see Materials and Methods and section S1), so that the dipolar field is “decoupled” (25); that is, the resultant field is nearly parallel to the muon spin, and the dipolar fields do not cause appreciable muon precession. Thus, one observes only dynamic relaxation.

The results are shown in Fig. 1, together with fits of Eq. 1 to the data. The rates are very small, close to the lower limit accessible to the technique, and the statistical uncertainty is large. Control experiments and precautions taken to minimize systematic errors are discussed in section S2.

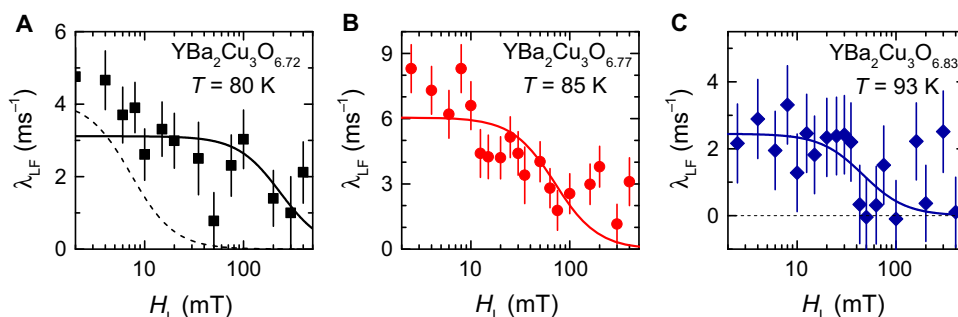
In Fig. 1 (A and B), the data lie above the fits for  $H_L \lesssim 5 \text{ mT}$ . This might suggest a logarithmic field dependence as an empirical description of the data. However, there is no clear physical mechanism for this in  $\text{YBa}_2\text{Cu}_3\text{O}_y$ . In highly anisotropic tetracyanoquinodimethane (TCNQ) charge transfer salts, nuclear spin relaxation due to diffusion of electronic spin quasi-particles exhibits  $\log H$  behavior for particular values of the anisotropic hopping rates (27). However, there is no reason to suspect this diffusive conduction in cuprates, and the higher low-field rates in Fig. 1 are more likely to be due to incomplete decoupling for these fields.

Table 1 gives values of  $\tau_c$  and  $B_{loc}^{rms}$  from the fits, together with 1 standard deviation (SD) ( $1 \sigma$ ) statistical uncertainties. The experimental values of  $B_{loc}^{rms}$  differ from zero by 5 to 9  $\sigma$  individually and  $\sim 10 \sigma$  cumulatively; nonzero values are established at this level. Both  $\tau_c$  and  $B_{loc}^{rms}$  vary smoothly with  $y$ . We carried out dipolar lattice sum calculations for  $B_{loc}$ , assuming candidate muon stopping sites from the literature (28, 29) and approximating the current loops as point dipoles (30). These yield estimates  $B_{loc} \approx 1$  to  $1.5 \text{ mT}$  for  $0.1$ - $\mu\text{B}$  loop-current magnetic moments, of the same order of magnitude as the observed values. The calculated values are not changed significantly for the “criss-cross” bilayer loop-current configurations recently reported by Mangin-Thro *et al.* (31).

It is evident that  $\tau_c$  falls in the middle of the range of experimental consistency discussed above. The observed increase of  $\tau_c$  with increasing  $y$  could be due to the approach to a quantum critical point as  $T_{mag} \rightarrow 0$ . However, fluctuations of the short-range IUC magnetic order may be associated with defects (21), in which case  $\tau_c$  could depend on sample preparation and not be an intrinsic property. More work is required to elucidate the nature of the observed fluctuations.

Exponential relaxation is observed in ZF together with the expected Gaussian contribution due to random quasi-static dipolar fields from nuclear moments (compare section S1). Just above  $T_c$ ,  $\lambda_{ZF}$  for  $y = 6.72$  (Fig. 2A) is a factor of about 5 higher than  $\lambda_{LF}$  above  $T_c$  (Fig. 1A). Some of this increase is due to a Lorentzian contribution to the distribution of static fields (13), but some of it is doubtless because of dynamic relaxation; in ZF, the two are hard to disentangle experimentally (section S1).

The temperature dependence of  $\lambda$  was measured in ZF and LF ( $H_L = 4 \text{ mT}$ ) for various samples. Figure 2 (A and B) shows  $\lambda_{ZF}(T)$  and  $\lambda_{LF}(T)$ , respectively, for  $y = 6.72$ , Fig. 2C shows  $\lambda_{LF}(T)$  for  $y = 6.77$ , and Fig. 2D



**Fig. 1. Dependence of the LF exponential relaxation rate  $\lambda_{LF}(H_L)$  on LF  $H_L$  in  $\text{YBa}_2\text{Cu}_3\text{O}_y$ .** (A)  $y = 6.72$ ,  $T = 80 \text{ K}$ . (B)  $y = 6.77$ ,  $T = 85 \text{ K}$ . (C)  $y = 6.83$ ,  $T = 93 \text{ K}$ . Curves: Fits of Eq. 1 to the data. A fit for  $y = 6.72$  using Eq. 1 with  $\tau_c$  fixed at one order larger than the optimal fit result [ $\tau_c = 5$  (2) ns] is plotted in (A) (dashed curve) for comparison of fit quality.

**Table 1. Correlation times  $\tau_c$  and rms muon local fields  $B_{\text{loc}}^{\text{rms}}$  from muon spin relaxation rates in  $\text{YBa}_2\text{Cu}_3\text{O}_y$ .**

$y$	Temperature (K)	$\tau_c$ (ns)	$B_{\text{loc}}^{\text{rms}}$ (mT)
6.72	80	5(2)	0.92(19)
6.77	85	10(3)	0.87(10)
6.83	93	25(10)	0.37(6)

shows  $\lambda_{\text{ZF}}(T)$  for  $y = 6.95$ . Maxima at  $T_{\text{mag}} \approx T^*$  and low-temperature increases are observed in all samples and fields, the former with statistical significance levels of 4 to 5  $\sigma$  individually and  $\sim 8 \sigma$  cumulatively (see Materials and Methods). A relaxation rate maximum is often observed at second-order magnetic transitions (32), associated with critical slowing down of magnetic fluctuations near  $T_{\text{mag}}$ . However, the low-temperature increase is unusual and is discussed below in more detail.

In the phase diagram of Fig. 3,  $T_{\text{mag}}$  from our  $\mu\text{SR}$  data is plotted versus the hole concentration  $p$  (and the oxygen content  $y$ ) along with  $T_c$  and  $T^*$  from other experiments. Values of  $T_{\text{mag}}$  are consistent with results of other experiments: polarized neutron diffraction (5, 6), terahertz birefringence (7), resonant ultrasound (33), and second harmonic generation (8). [ $T^*$  is also the temperature around which changes in transport properties (34) and thermodynamic properties (35, 36) from those of the strange metal phase begin to be observed.] The observed  $T_{\text{mag}}$  also corresponds well to the results of recent torque magnetometry measurements, which support a second-order phase transition at  $T^*$  (9). The inset of Fig. 3 compares the doping dependence of the square root  $J_{\text{neu}}^{1/2}$  of the polarized neutron diffraction cross section (37) with that of  $B_{\text{loc}}^{\text{rms}}$ . These quantities are both proportional to the order parameter for IUC magnetic order, and they follow the same trend.

## DISCUSSION

The observed increase of motionally narrowed muon spin relaxation with decreasing temperature below  $T^*$ , shown in Fig. 2, cannot occur in a transition to a uniform ordered state. It is, however, consistent with low-frequency fluctuations in domains of IUC magnetic order, of increasing magnitude with the increasing order parameter (21). Scanning tunneling spectroscopy experiments (22) have found these domains in the pseudogap phase associated with defects, with linear dimensions of  $\sim 20$  unit cells; these provide a mechanism for the pseudogap in the one-particle spectra (21). Other experiments (38, 39) have observed mysterious anomalous low-frequency fluctuations in the pseudogap phase ascribed to extended defects.

Phenomena other than IUC magnetism can affect  $\mu\text{SR}$  experiments. Sonier and co-workers (14, 16) observed features in ZF data from  $\text{YBa}_2\text{Cu}_3\text{O}_y$ , and attributed them to charge and structural inhomogeneities from lattice changes and CDW formation. Fits of an exponentially damped Gaussian Kubo-Toyabe (KT) to data from a nearly fully doped sample ( $y = 6.985$ ) (14) yielded correlations between  $\Delta(T)$  and  $\lambda(T)$ , leading to the conclusion that the exponential rate could not be determined unambiguously (40). Structure in ZF  $\lambda(T)$  with  $\Delta(T)$  held fixed was related to the onset of short-range CDW order (41) for that doping.

For slightly lower doping ( $y = 6.95$ ), however, fits with  $\Delta(T)$  a free parameter (42) yield a clear peak in  $\lambda(T)$  at  $T_{\text{mag}} = 80$  K with no corresponding structure in  $\Delta(T)$  at that temperature (compare section

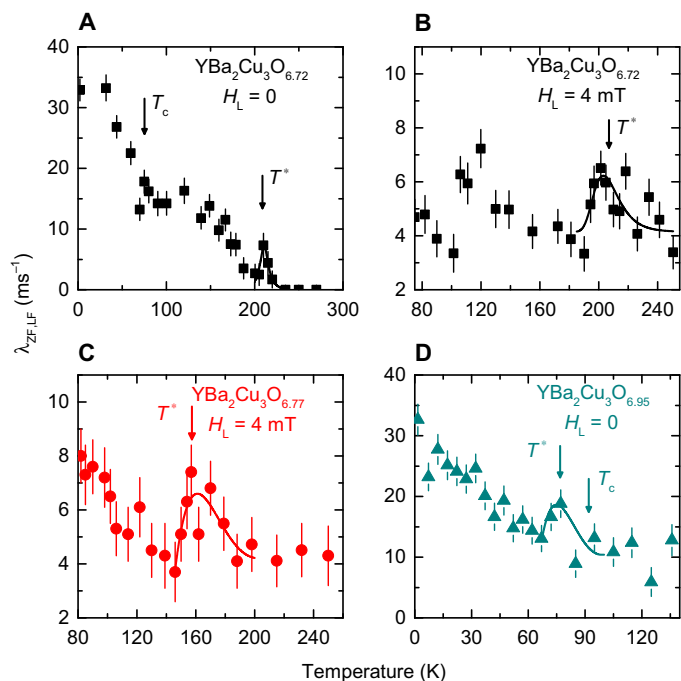


**Fig. 2. Temperature dependence of the dynamic muon relaxation rate  $\lambda$  in  $\text{YBa}_2\text{Cu}_3\text{O}_y$ .** (A)  $y = 6.72$ , LF  $H_L = 0$ . (B)  $y = 6.72$ ,  $\mu_0 H_L = 4$  mT. (C)  $y = 6.77$ ,  $\mu_0 H_L = 4$  mT, (D)  $y = 6.95$ ,  $H_L = 0$ . The pseudogap onset temperature  $T^*$  is shown for each doping.

S3). NQR measurements (43) on a sample of similar oxygen content showed that CDW order sets in at a considerably lower temperature ( $\sim 35$  K). For  $y < 6.95$ , ZF CDW transition temperatures from NMR/NQR and other measurements are significantly lower than  $T_{\text{mag}}$  from our experiments. For all  $y$ , the onset of long-range CDW order is at still lower temperatures and is only observed in high-applied magnetic fields (20). Recent torque magnetometry measurements also provide strong evidence that CDW order and the pseudogap phase are characterized by distinct broken symmetries at different temperatures (9). The detailed temperature-doping phase diagram (Fig. 3) shows that lattice change/CDW and pseudogap phases set in at distinct temperatures and are distinct phenomena. We conclude that there is no evidence for associating the maxima in  $\lambda(T)$  and its increase at low temperatures with either CDW or charge inhomogeneity.

It has been claimed (40) that the maxima for  $y = 6.72$  and  $6.77$  at  $\sim 210$  and  $\sim 165$  K, respectively (Fig. 2, A and C), could be due to the onset of thermally activated muon hopping (diffusion) (14); this causes unwanted dynamic relaxation by nuclear dipolar fields. However, in the usual trapping-detrapping scenario (44), the maximum is due to a temperature sequence in which the muons are trapped and static at low temperatures, begin hopping with increasing temperature, find deep impurity traps and become static again at an intermediate temperature, and finally detrapp definitively at high temperatures. It has been argued (42) that this is highly unlikely in the present case because independent  $\mu\text{SR}$  determinations (14, 42, 45) of the muon hopping rate using dynamic Gaussian KT fits (25) show that hopping is too slow to produce the observed decrease in  $\lambda(T)$  below the maximum (compare section S4). Alternatively, the maximum might be purely dynamic because with increasing temperature, the muon hopping rate passes through the muon Zeeman frequency. In that case, however, the application of  $H_L = 4$  mT field would move the maximum to temperatures where the hopping rate is  $\sim \gamma_\mu H_L = 3.4 \mu\text{s}^{-1}$ . According to the dynamic KT fits, this

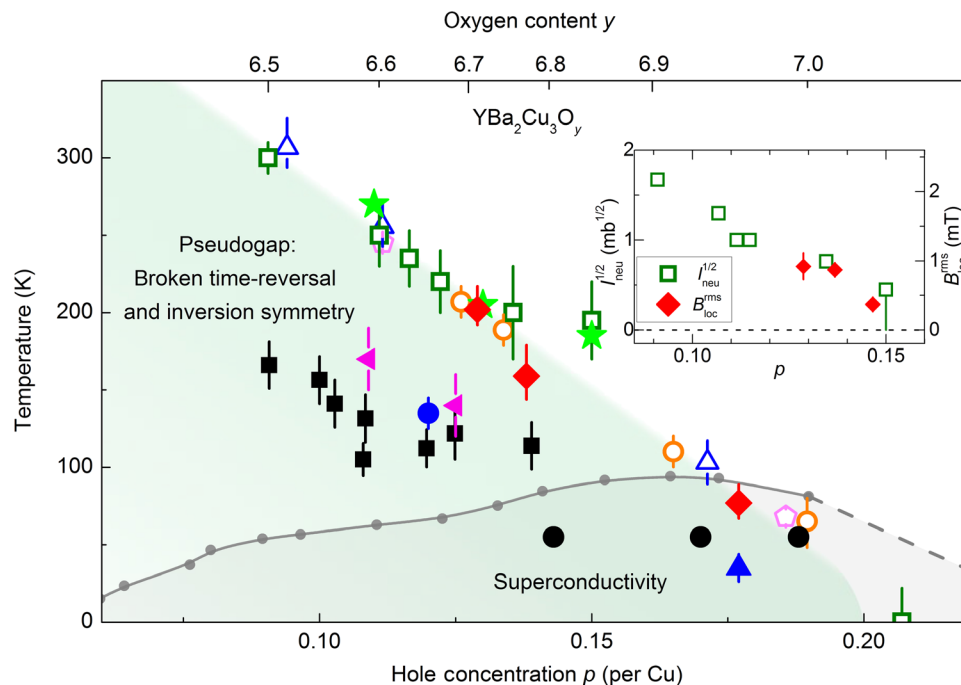


**Fig. 3. Phase diagram of pseudogap and charge-density-wave/charge inhomogeneity onset temperatures in  $\text{YBa}_2\text{Cu}_3\text{O}_y$ .** Red diamonds: Temperatures  $T_{\text{mag}}$  of maxima in  $\mu\text{SR}$  exponential relaxation rates (Fig. 2). Open green squares: Pseudogap temperatures  $T^*$  from polarized neutron diffraction (5, 6). Open blue triangles:  $T^*$  from THz birefringence (7). Pink pentagons:  $T^*$  from resonant ultrasound (33). Orange circles:  $T^*$  from second harmonic generation (8). Green stars:  $T^*$  from magnetic torque (9). Magenta left triangles: Charge-density-wave (CDW) onset temperatures  $T_{\text{CDW}}$  from NMR (20). Filled blue triangle:  $T_{\text{CDW}}$  from nuclear quadrupole resonance (NQR) (43). Black squares:  $T_{\text{CDW}}$  from Hall effect (53). Blue circle:  $T_{\text{CDW}}$  from high-energy x-ray diffraction (54). Black circles: Onset of “charge inhomogeneity” (CDW or lattice change) from  $\mu\text{SR}$  experiments (14). Gray points: Superconducting transition temperatures. Inset: Doping dependences of the square root  $I_{\text{neu}}^{1/2}$  of the polarized neutron diffraction cross section (37) and the rms magnitude  $B_{\text{loc}}^{\text{rms}}$  of the fluctuating local field (Table 1).

is well above 300 K, whereas in our data (Fig. 2B), the position of the maximum is unchanged. We conclude that muon hopping is not the origin of the maximum for  $y = 6.72$ . Note that, for  $y = 6.67$ , no maximum in  $\lambda_{\text{ZF}}(T)$  was seen near  $T^* \sim 200$  K (13), which is probably due to significant muon hopping at this temperature.

Previous transverse-field (TF)  $\mu\text{SR}$  experiments in the pseudogap phase (46) observed exponential relaxation and ascribed it to static spatial inhomogeneity of superconducting fluctuations. Our observed LF- $\mu\text{SR}$  rates (Fig. 1) are an order of magnitude slower than the TF- $\mu\text{SR}$  rates. This is consistent with the assumption that the latter are static and precludes detecting the dynamic relaxation in TF- $\mu\text{SR}$ .

The observed critical slowing down at  $T_{\text{mag}} \approx T^*$  (Fig. 2) indicates that this temperature marks the onset of broken time-reversal symmetry, as is also found in each of the four hole-doped cuprate families amenable so far to polarized neutron diffraction experiments. The observed magnitude of the order parameter of about  $0.1\mu_{\text{B}}$  staggered moment per unit cell has a condensation energy of  $\sim 50$  J/mol, similar to the maximum superconducting energy in cuprates (47). These properties are all consistent with our results. Note that a recent LF- $\mu\text{SR}$  study of  $\text{Bi}_{2+x}\text{Sr}_{2-x}\text{CaCu}_2\text{O}_{8+\delta}$  (45) also reported a quasi-static internal magnetic field in the pseudogap phase.

Our discovery of fluctuating magnetic fields provides an understanding of the absence of static magnetic fields due to IUC magnetic order in  $\text{YBa}_2\text{Cu}_3\text{O}_y$ . The expected fields are present but fluctuating. Although  $\mu\text{SR}$  is a point probe in real space and, thus, is not directly sensitive to the spatial symmetry, our results are strong evidence for IUC order and its excitations and establish them as important for understanding the unusual behavior of cuprates.

## MATERIALS AND METHODS

### Sample growth and characterization

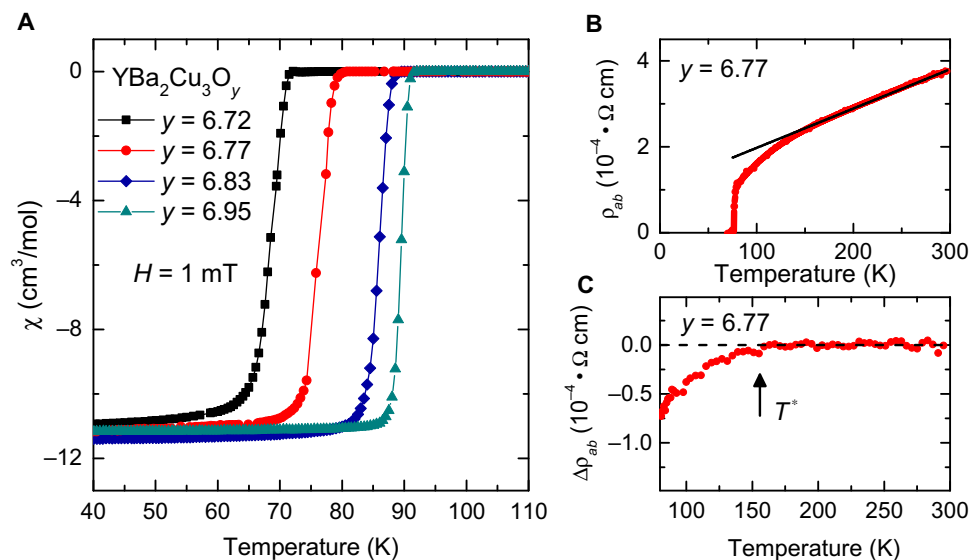
High-quality single crystals of  $\text{YBa}_2\text{Cu}_3\text{O}_y$  were grown by the top-seeded solution growth polythermal method using  $3\text{BaO}-5\text{CuO}$  solvent (48). A  $\text{YBa}_2\text{Cu}_3\text{O}_y$  single crystal with an  $ab$  plane area of  $10\text{ mm} \times 10\text{ mm}$  and  $c$  axis length of  $8\text{ mm}$  was synthesized with a cooling rate of  $0.5\text{ K}$  per hour in air. The crystal was then cut into small pellets with thicknesses of  $0.55\text{ mm}$  and lateral dimensions of  $2\text{ mm} \times 2\text{ mm}$ . Single crystals with optimal  $T_c = 91\text{ K}$  were achieved by annealing at  $400^\circ\text{C}$  for 180 hours in flowing oxygen. A range of oxygen concentrations of  $\text{YBa}_2\text{Cu}_3\text{O}_y$  was achieved by post-annealing in flowing oxygen at different temperatures as described in the study by Gao *et al.* (49), resulting in superconducting transition temperatures between 72 and 88 K.

Figure 4 shows the temperature dependences of the magnetization and the resistivity in our samples. The data indicate that the superconducting transitions are sharp. The values of  $T^*$  from the departure of the resistivity from linearity are in agreement with previous results (50).

### Muon spin relaxation experiments

In the time differential  $\mu\text{SR}$  technique (51), spin-polarized muons are implanted into the sample. In the muon decay to a positron and two neutrinos, the positron momentum is preferentially oriented along the direction of the muon spin at the time of decay. The time evolution of the ensemble muon polarization can therefore be monitored via the asymmetry in positron emission count rates.

Our  $\mu\text{SR}$  experiments were performed using the Los Alamos Meson Physics Facility spectrometer at the M20 beamline of TRIUMF (Vancouver, Canada) and the MUSR and EMU spectrometers at ISIS, Rutherford



**Fig. 4. Characterization data from YBa<sub>2</sub>Cu<sub>3</sub>O<sub>y</sub> single crystals.** (A) Magnetization of YBa<sub>2</sub>Cu<sub>3</sub>O<sub>y</sub>,  $y = 6.72, 6.77, 6.83,$  and  $6.95,$  showing sharp superconducting transitions. (B) Temperature dependence of electrical resistivity  $\rho_{ab}$  for  $y = 6.77$  showing a deviation from linearity. (C) Temperature dependence of the deviation  $\Delta\rho_{ab}$  from linear resistivity for  $y = 6.77$ . The deviation sets in below  $T^* = 156$  K, which is consistent with reported results (50).

**Table 2. IRSDs of  $B_{loc}^{rms}$  and relaxation rate maxima near  $T_{mag}$  from muon spin relaxation rates in YBa<sub>2</sub>Cu<sub>3</sub>O<sub>y</sub>.**

$y$	$B_{loc}^{rms}$		Relaxation rate maxima (Fig. 2)	
	IRSD	$H_L$ (mT)	No. of points	IRSD
6.72	4.8	0	7	4.5
6.72		4	11	3.8
6.77	8.7	4	15	5.2
6.83	6.2			
6.95		0	6	3.9
Cumulative	11.7			8.8

Appleton Laboratory (Chilton, United Kingdom). At both facilities, muons were implanted into the sample with their initial spin polarization  $P_\mu$  perpendicular to the  $ab$  plane.

Appropriate functional forms, discussed in section S1, were least-squares fit to the asymmetry data using the MUSRFIT  $\mu$ SR analysis program (52). The LF rates were very low and were near the resolution limit of the technique. The difference between the rates was small but was resolved. Note that  $\lambda_{LF}$  in Bi<sub>2+x</sub>Sr<sub>2-x</sub>CaCu<sub>2</sub>O<sub>8+ $\delta$</sub>  is also quite small for  $H_L > 1$  mT (45). To our knowledge, no LF- $\mu$ SR data for other cuprate superconductors in comparable fields have been reported. We nevertheless speculate that the scatter in Fig. 1 was typical for the hole-doped superconducting cuprate family.

### Statistical analysis

Random error in  $\mu$ SR experiments arises from the Poisson distribution of positron count rates. The MUSRFIT analysis software computes the propagation of this error to that of the parameters of the fit function and reports their probable SD  $\sigma$ . All parameter uncertainties quoted in this article are  $1\sigma$ .

The inverse relative SDs (IRSDs) (the  $N$  in “ $N\sigma$ ”) for  $B_{loc}^{rms}$  (Table 1) and for the maxima in the temperature dependences at  $T_{mag}$  (Fig. 3) are shown in Table 2. The IRSD for  $B_{loc}^{rms}$  is simply its value divided by its SD. For the maxima at  $T_{mag}$ , baseline points were chosen above and below each maximum, and baseline values at intermediate points were estimated by linear interpolation. The IRSD of each point is its amplitude relative to the baseline divided by its SD, and the IRSD of the maximum is the square root of the sum of squares of the IRSDs of the points. The sign of the amplitude was included in this sum to account for negative contributions. For both  $B_{loc}^{rms}$  and the maxima, the cumulative IRSD is the square root of the sum of squares of the individual sample IRSDs. It can be seen that some individual IRSDs are marginal, but the cumulative values are quite satisfactory.

### SUPPLEMENTARY MATERIALS

Supplementary material for this article is available at <http://advances.sciencemag.org/cgi/content/full/4/1/eaao5235/DC1>

- section S1. Muon relaxation functions
  - section S2. Control experiments
  - section S3. Temperature dependence of static Gaussian KT relaxation rate  $\Delta_{ZF}(T)$
  - section S4. Muon hopping, superconductivity
  - section S5. Superconducting fluctuations
  - section S6. High-temperature relaxation
  - fig. S1. ZF relaxation of the muon asymmetry  $A_\mu(t)$  in YBa<sub>2</sub>Cu<sub>3</sub>O<sub>6.72</sub>.
  - fig. S2. Time evolution of the positron count rate asymmetry  $A_\mu$  at various temperatures and fields in single-crystal YBa<sub>2</sub>Cu<sub>3</sub>O<sub>y</sub>.
  - fig. S3. LF muon spin relaxation rates in silver samples.
  - fig. S4. Fits of representative ZF- $\mu$ SR spectra from YBa<sub>2</sub>Cu<sub>3</sub>O<sub>6.95</sub> for  $\Delta_{ZF}$  fixed and free.
  - fig. S5. Temperature dependence of ZF exponential damping rate  $\lambda_{ZF}$  and static Gaussian KT rate  $\Delta_{ZF}$  for YBa<sub>2</sub>Cu<sub>3</sub>O<sub>6.95</sub>.
  - fig. S6. Damped dynamic Gaussian KT fit of ZF data from YBa<sub>2</sub>Cu<sub>3</sub>O<sub>6.72</sub>.
- References (55–58)

### REFERENCES AND NOTES

1. T. Timusk, B. Statt, The pseudogap in high-temperature superconductors: An experimental survey. *Rep. Prog. Phys.* **62**, 61–122 (1999).
2. M. R. Norman, C. Pépin, The electronic nature of high temperature cuprate superconductors. *Rep. Prog. Phys.* **66**, 1547–1610 (2003).

3. M. R. Norman, D. Pines, C. Kallin, The pseudogap: Friend or foe of high  $T_c$ ? *Adv. Phys.* **54**, 715–733 (2005).
4. B. Keimer, S. A. Kivelson, M. R. Norman, S. Uchida, J. Zaanen, From quantum matter to high-temperature superconductivity in copper oxides. *Nature* **518**, 179–186 (2015).
5. B. Fauqué, Y. Sidis, V. Hinkov, S. Pailhès, C. T. Lin, X. Chaud, P. Bourges, Magnetic order in the pseudogap phase of high- $T_c$  superconductors. *Phys. Rev. Lett.* **96**, 197001 (2006).
6. L. Mangin-Thro, Y. Sidis, A. Wildes, P. Bourges, Intra-unit-cell magnetic correlations near optimal doping in  $\text{YBa}_2\text{Cu}_3\text{O}_{6.85}$ . *Nat. Commun.* **6**, 7705 (2015).
7. Y. Lubashevsky, L. Pan, T. Kirzhner, G. Koren, N. P. Armitage, Optical birefringence and dichroism of cuprate superconductors in the THz regime. *Phys. Rev. Lett.* **112**, 147001 (2014).
8. L. Zhao, C. A. Belvin, R. Liang, D. A. Bonn, W. N. Hardy, N. P. Armitage, D. Hsieh, A global in-plane-symmetry-broken phase inside the pseudogap region of  $\text{YBa}_2\text{Cu}_3\text{O}_y$ . *Nat. Phys.* **13**, 250–254 (2016).
9. Y. Sato, S. Kasahara, H. Murayama, Y. Kasahara, E.-G. Moon, T. Nishizaki, T. Loew, J. Porras, B. Keimer, T. Shibauchi, Y. Matsuda, Thermodynamic evidence for a nematic phase transition at the onset of the pseudogap in  $\text{YBa}_2\text{Cu}_3\text{O}_y$ . *Nat. Phys.* **13**, 1074–1078 (2017).
10. C. Varma, High-temperature superconductivity: Mind the pseudogap. *Nature* **468**, 184–185 (2010).
11. A. S. Moskvin, Pseudogap phase in cuprates: Oxygen orbital moments instead of circulating currents. *JETP Lett.* **96**, 385–390 (2012).
12. M. Fechner, M. J. A. Fierz, F. Thöle, U. Staub, N. A. Spaldin, Quasistatic magnetoelectric multipoles as order parameter for pseudogap phase in cuprate superconductors. *Phys. Rev. B* **93**, 174419 (2016).
13. J. E. Sonier, J. H. Brewer, R. F. Kiefl, R. I. Miller, G. D. Morris, C. E. Stronach, J. S. Gardner, S. R. Dunsiger, D. A. Bonn, W. N. Hardy, R. Liang, R. H. Heffner, Anomalous weak magnetism in superconducting  $\text{YBa}_2\text{Cu}_3\text{O}_{6+x}$ . *Science* **292**, 1692–1695 (2001).
14. J. E. Sonier, J. H. Brewer, R. F. Kiefl, R. H. Heffner, K. F. Poon, S. L. Stubbs, G. D. Morris, R. I. Miller, W. N. Hardy, R. Liang, D. A. Bonn, J. S. Gardner, C. E. Stronach, N. J. Curro, Correlations between charge ordering and local magnetic fields in overdoped  $\text{YBa}_2\text{Cu}_3\text{O}_{6+x}$ . *Phys. Rev. B* **66**, 134501 (2002).
15. G. J. MacDougall, A. A. Aczel, J. P. Carlo, T. Ito, J. Rodriguez, P. L. Russo, Y. J. Uemura, S. Wakimoto, G. M. Luke, Absence of broken time-reversal symmetry in the pseudogap state of the high temperature  $\text{La}_{2-x}\text{Sr}_x\text{CuO}_4$  superconductor from muon-spin-relaxation measurements. *Phys. Rev. Lett.* **101**, 017001 (2008).
16. J. E. Sonier, V. Pacradouni, S. A. Sabok-Sayr, W. N. Hardy, D. A. Bonn, R. Liang, H. A. Mook, Detection of the unusual magnetic orders in the pseudogap region of a high-temperature superconducting  $\text{YBa}_2\text{Cu}_3\text{O}_{6.6}$  crystal by muon-spin relaxation. *Phys. Rev. Lett.* **103**, 167002 (2009).
17. W. Huang, V. Pacradouni, M. P. Kennett, S. Komiya, J. E. Sonier, Precision search for magnetic order in the pseudogap regime of  $\text{La}_{2-x}\text{Sr}_x\text{CuO}_4$  by muon spin relaxation. *Phys. Rev. B* **85**, 104527 (2012).
18. A. Pal, Investigation of potential fluctuating intra-unit cell magnetic order in cuprates by  $\mu\text{SR}$ . *Phys. Rev. B* **94**, 134514 (2016).
19. A. M. Mounce, S. Oh, J. A. Lee, W. P. Halperin, A. P. Reyes, P. L. Kuhns, M. K. Chan, C. Dorow, L. Ji, D. Xia, X. Zhao, M. Greven, Absence of static loop-current magnetism at the apical oxygen site in  $\text{HgBa}_2\text{CuO}_{4.8}$  from NMR. *Phys. Rev. Lett.* **111**, 187003 (2013).
20. T. Wu, H. Mayaffre, S. Krämer, M. Horvatić, C. Berthier, W. N. Hardy, R. Liang, D. A. Bonn, M.-H. Julien, Incipient charge order observed by NMR in the normal state of  $\text{YBa}_2\text{Cu}_3\text{O}_y$ . *Nat. Commun.* **6**, 6438 (2015).
21. C. M. Varma, Pseudogap in cuprates in the loop-current ordered state. *J. Phys. Condens. Matter* **26**, 505701 (2014).
22. K. Fujita, A. R. Schmidt, E.-A. Kim, M. J. Lawler, D. H. Lee, J. C. Davis, H. Eisaki, S.-i. Uchida, Spectroscopic imaging scanning tunneling microscopy studies of electronic structure in the superconducting and pseudogap phases of cuprate high- $T_c$  superconductors. *J. Phys. Soc. Jpn.* **81**, 0111005 (2012).
23. Y. Itoh, T. Machi, A. Yamamoto, Ultraslow fluctuations in the pseudogap states of  $\text{HgBa}_2\text{CaCu}_2\text{O}_{6+\delta}$ . *Phys. Rev. B* **95**, 094501 (2017).
24. C. P. Slichter, *Principles of Magnetic Resonance* (Springer, 1996).
25. R. S. Hayano, Y. J. Uemura, J. Imazato, N. Nishida, T. Yamazaki, R. Kubo, Zero- and low-field spin relaxation studied by positive muons. *Phys. Rev. B* **20**, 850–859 (1979).
26. Y. Aoki, A. Tsuchiya, T. Kanayama, S. R. Saha, H. Sugawara, H. Sato, W. Higemoto, A. Koda, K. Ohishi, K. Nishiyama, R. Kadono, Time-reversal symmetry-breaking superconductivity in heavy-fermion  $\text{PrO}_4\text{Sb}_{12}$  detected by muon-spin relaxation. *Phys. Rev. Lett.* **91**, 067003 (2003).
27. M. A. Butler, L. R. Walker, Z. G. Soos, Dimensionality of spin fluctuations in highly anisotropic TCNQ salts. *J. Chem. Phys.* **64**, 3592–3601 (1976).
28. N. Nishida, H. Miyatake, Positive muon sites and possibility of anyons in the  $\text{YBa}_2\text{Cu}_3\text{O}_x$  system. *Hyperfine Interact.* **63**, 183–197 (1991).
29. M. Weber, P. Birrer, F. N. Gygax, B. Hitti, E. Lippelt, H. Maletta, A. Schenck, Identification of  $\mu^+$ -sites in the 1-2-3 compound. *Hyperfine Interact.* **63**, 207–212 (1991).
30. A. Shekhter, L. Shu, V. Aji, D. E. MacLaughlin, C. M. Varma, Screening of point charge impurities in highly anisotropic metals: Application to  $\mu^+$ -spin relaxation in underdoped cuprate superconductors. *Phys. Rev. Lett.* **101**, 227004 (2008).
31. L. Mangin-Thro, Y. Li, Y. Sidis, P. Bourges,  $a$ - $b$  Anisotropy of the intra-unit-cell magnetic order in  $\text{YBa}_2\text{Cu}_3\text{O}_{6.6}$ . *Phys. Rev. Lett.* **118**, 097003 (2017).
32. P. Dalmas de Réotier, A. Yaouanc, Muon spin rotation and relaxation in magnetic materials. *J. Phys. Condens. Matter* **9**, 9113–9166 (1997).
33. A. Shekhter, B. J. Ramshaw, R. Liang, W. N. Hardy, D. A. Bonn, F. F. Balakirev, R. D. McDonald, J. B. Betts, S. C. Riggs, A. Migliori, Bounding the pseudogap with a line of phase transitions in  $\text{YBa}_2\text{Cu}_3\text{O}_{6+\delta}$ . *Nature* **498**, 75–77 (2013).
34. R. Daou, J. Chang, D. LeBoeuf, O. Cyr-Choinière, F. Laliberté, N. Doiron-Leyraud, B. J. Ramshaw, R. Liang, D. A. Bonn, W. N. Hardy, L. Taillefer, Broken rotational symmetry in the pseudogap phase of a high- $T_c$  superconductor. *Nature* **463**, 519–522 (2010).
35. J. W. Loram, J. Luo, J. R. Cooper, W. Y. Liang, J. L. Tallon, Evidence on the pseudogap and condensate from the electronic specific heat. *J. Phys. Chem. Solids* **62**, 59–64 (2001).
36. B. Leridon, P. Monod, D. Colson, A. Forget, Thermodynamic signature of a phase transition in the pseudogap phase of  $\text{YBa}_2\text{Cu}_3\text{O}_x$  high- $T_c$  superconductor. *Europhys. Lett.* **87**, 17011 (2009).
37. Y. Li, V. Balédent, N. Barišić, Y. Cho, B. Fauqué, Y. Sidis, G. Yu, X. Zhao, P. Bourges, M. Greven, Unusual magnetic order in the pseudogap region of the superconductor  $\text{HgBa}_2\text{CuO}_{4+\delta}$ . *Nature* **455**, 372–375 (2008).
38. J. Corson, J. Orenstein, S. Oh, J. O'Donnell, J. N. Eckstein, Nodal quasiparticle lifetime in the superconducting state of  $\text{Bi}_2\text{Sr}_2\text{CaCu}_2\text{O}_{8+\delta}$ . *Phys. Rev. Lett.* **85**, 2569–2572 (2000).
39. R. Harris, P. J. Turner, S. Kamal, A. R. Hosseini, P. Dossanjh, G. K. Mullins, J. S. Bobowski, C. P. Bidinosti, D. M. Broun, R. Liang, W. N. Hardy, D. A. Bonn, Phenomenology of  $d$ -axis and  $b$ -axis charge dynamics from microwave spectroscopy of highly ordered  $\text{YBa}_2\text{Cu}_3\text{O}_{6.50}$  and  $\text{YBa}_2\text{Cu}_3\text{O}_{6.993}$ . *Phys. Rev. B* **74**, 104508 (2006).
40. J. E. Sonier, Comment on “Discovery of slow magnetic fluctuations and critical slowing down in the pseudogap phase of  $\text{YBa}_2\text{Cu}_3\text{O}_y$ ,” <https://arxiv.org/abs/1706.03023> (2017).
41. B. Grévin, Y. Berthier, G. Collin, In-plane charge modulation below  $T_c$  and charge-density-wave correlations in the chain layer in  $\text{YBa}_2\text{Cu}_3\text{O}_7$ . *Phys. Rev. Lett.* **85**, 1310–1313 (2000).
42. J. Zhang, Z. F. Ding, C. Tan, K. Huang, O. O. Bernal, P.-C., Ho, G. D. Morris, A. D. Hillier, P. K. Biswas, S. P. Cottrell, H. Xiang, X. Yao, D. E. MacLaughlin, L. Shu, Reply to “Comment on ‘Discovery of slow magnetic fluctuations and critical slowing down in the pseudogap phase of  $\text{YBa}_2\text{Cu}_3\text{O}_y$ ,’” <https://arxiv.org/abs/1707.00069> (2017).
43. S. Krämer, M. Mehring, Krämer and Mehring reply. *Phys. Rev. Lett.* **84**, 1637 (2000).
44. C. Boekema, R. H. Heffner, R. L. Hutson, M. Leon, M. E. Schillaci, W. J. Kossler, M. Numan, S. A. Dods, Diffusion and trapping of positive muons in niobium. *Phys. Rev. B* **26**, 2341–2348 (1982).
45. A. Pal, S. R. Dunsiger, K. Akintola, A. C. Y. Fang, A. Elhosary, M. Ishikado, H. Eisaki, J. E. Sonier, Quasi-static internal magnetic field detected in the pseudogap phase of  $\text{Bi}_{2-x}\text{Sr}_{2-x}\text{CaCu}_2\text{O}_{8+\delta}$  by  $\mu\text{SR}$ . <https://arxiv.org/abs/1707.01111> (2017).
46. Z. L. Mahyari, A. Cannell, E. V. L. de Mello, M. Ishikado, H. Eisaki, R. Liang, D. A. Bonn, J. E. Sonier, Universal inhomogeneous magnetic-field response in the normal state of cuprate high- $T_c$  superconductors. *Phys. Rev. B* **88**, 144504 (2013).
47. C. M. Varma, L. Zhu, Specific heat and sound velocity at the relevant competing phase of high temperature superconductors. *Proc. Natl. Acad. Sci. U.S.A.* **112**, 6331–6335 (2015).
48. H. Xiang, L. Guo, H. Li, X. Cui, J. Qian, G. Hussain, Y. Liu, X. Yao, Q. Rao, Z. Q. Zou, Polythermal method of top-seeded solution-growth for large-sized single crystals of  $\text{REBa}_2\text{Cu}_3\text{O}_{7-\delta}$ . *Scr. Mater.* **116**, 36–39 (2016).
49. H. Gao, C. Ren, L. Shan, Y. Wang, Y. Zhang, S. Zhao, X. Yao, H.-H. Wen, Reversible magnetization and critical fluctuations in systematically doped  $\text{YBa}_2\text{Cu}_3\text{O}_{7-\delta}$  single crystals. *Phys. Rev. B* **74**, 020505 (2006).
50. Y. Ando, S. Komiya, K. Segawa, S. Ono, Y. Kurita, Electronic phase diagram of high- $T_c$  cuprate superconductors from a mapping of the in-plane resistivity curvature. *Phys. Rev. Lett.* **93**, 267001 (2004).
51. A. Yaouanc, P. Dalmas de Réotier, *Muon Spin Rotation, Relaxation, and Resonance: Applications to Condensed Matter* (International Series of Monographs on Physics, Oxford Univ. Press, 2011).
52. A. Suter, B. M. Wojek, Musrfit: A free platform-independent framework for  $\mu\text{SR}$  data analysis. *Phys. Procedia* **30**, 69–73 (2012).
53. D. LeBoeuf, N. Doiron-Leyraud, B. Vignolle, M. Sutherland, B. J. Ramshaw, J. Levallois, R. Daou, F. Laliberté, O. Cyr-Choinière, J. Chang, Y. J. Jo, L. Balicas, R. Liang, D. A. Bonn, W. N. Hardy, C. Proust, L. Taillefer, Lifshitz critical point in the cuprate superconductor  $\text{YBa}_2\text{Cu}_3\text{O}_y$  from high-field Hall effect measurements. *Phys. Rev. B* **83**, 054506 (2011).
54. J. Chang, E. Blackburn, A. T. Holmes, N. B. Christensen, J. Larsen, J. Mesot, R. Liang, D. A. Bonn, W. N. Hardy, A. Watenphul, M. Zimmermann, E. M. Forgan, S. M. Hayden, Direct observation of competition between superconductivity and charge density wave order in  $\text{YBa}_2\text{Cu}_3\text{O}_{6.67}$ . *Nat. Phys.* **8**, 871–876 (2012).
55. R. Kubo, T. Toyabe, in *Magnetic Resonance and Relaxation*, R. Blinc, Ed. (North-Holland, 1967), pp. 810–823.

56. A. Maisuradze, W. Schnelle, R. Khasanov, R. Gumeniuk, M. Nicklas, H. Rosner, A. Leithe-Jasper, Y. Grin, A. Amato, P. Thalmeier, Evidence for time-reversal symmetry breaking in superconducting  $\text{PrPt}_4\text{Ge}_{12}$ . *Phys. Rev. B* **82**, 024524 (2010).
57. J. F. Bueno, D. J. Arseneau, R. Bayes, J. H. Brewer, W. Faszler, M. D. Hasinoff, G. M. Marshall, E. L. Mathie, R. E. Mischke, G. D. Morris, K. Olchanski, V. Selivanov, R. Tacik, Longitudinal muon spin relaxation in high-purity aluminum and silver. *Phys. Rev. B* **83**, 205121 (2011).
58. O. Cyr-Choinière, R. Daou, F. Laliberté, C. Collignon, S. Badoux, D. LeBoeuf, J. Chang, B. J. Ramshaw, D. A. Bonn, W. N. Hardy, R. Liang, J.-Q. Yan, J.-G. Cheng, J.-S. Zhou, J. B. Goodenough, S. Pyon, T. Takayama, H. Takagi, N. Doiron-Leyraud, L. Taillefer, Pseudogap temperature  $T^*$  of cuprate superconductors from the Nernst effect, <https://arxiv.org/abs/1703.06927> (2017).

**Acknowledgments:** We are grateful to C. M. Varma for proposing these experiments and for numerous discussions. We thank the support teams at TRIUMF and ISIS for help during the experiments and J. H. Brewer for discussions and correspondence. **Funding:** The research performed in this study was partially supported by the National Key Research and Development Program of China (nos. 2016YFA0300503, 2017YFA0303104, and 2016YFA0300403), the National Natural Science Foundation of China (nos. 11774061 and 11474060), and the Science and Technology Commission of Shanghai Municipality of China (grant no. 15XD1500200). Research at University of California (UC), Riverside was supported by the UC Riverside Academic Senate. Work at California State University (CSU), Los Angeles was funded by NSF/

DMR (Division of Materials Research)/Partnerships for Research and Education in Materials-1523588. Research at CSU-Fresno was supported by NSF DMR-1506677.

**Author contributions:** L.S. and D.E.M. conceived the experiment and wrote the beam-time proposals. J.Z., Z.D., C.T., K.H., O.O.B., P.-C.H., G.D.M., A.D.H., P.K.B., S.P.C., D.E.M., and L.S. performed the  $\mu\text{SR}$  measurements, with D.E.M. and L.S. overseeing the experimental work. J.Z., H.X., and X.Y. grew the single-crystal samples. J.Z., D.E.M., and L.S. performed the data analysis; these authors wrote the manuscript. All authors discussed the data and contributed to the analysis. **Competing interests:** The authors declare that they have no competing interests. **Data and materials availability:** All data needed to evaluate the conclusions in the paper are present in the paper and/or the Supplementary Materials. Additional data related to this paper may be requested from the authors.

Submitted 10 August 2017

Accepted 30 November 2017

Published 5 January 2018

10.1126/sciadv.aao5235

**Citation:** J. Zhang, Z. Ding, C. Tan, K. Huang, O. O. Bernal, P.-C. Ho, G. D. Morris, A. D. Hillier, P. K. Biswas, S. P. Cottrell, H. Xiang, X. Yao, D. E. MacLaughlin, L. Shu, Discovery of slow magnetic fluctuations and critical slowing down in the pseudogap phase of  $\text{YBa}_2\text{Cu}_3\text{O}_y$ . *Sci. Adv.* **4**, eao5235 (2018).

## Discovery of slow magnetic fluctuations and critical slowing down in the pseudogap phase of $\text{YBa}_2\text{Cu}_3\text{O}_y$

Jian Zhang, Zhaofeng Ding, Cheng Tan, Kevin Huang, Oscar O. Bernal, Pei-Chun Ho, Gerald D. Morris, Adrian D. Hillier, Pabitra K. Biswas, Stephen P. Cottrell, Hui Xiang, Xin Yao, Douglas E. MacLaughlin and Lei Shu

*Sci Adv* 4 (1), eaao5235.  
DOI: 10.1126/sciadv.aao5235

### ARTICLE TOOLS

<http://advances.sciencemag.org/content/4/1/eaao5235>

### SUPPLEMENTARY MATERIALS

<http://advances.sciencemag.org/content/suppl/2017/12/22/4.1.eaao5235.DC1>

### REFERENCES

This article cites 51 articles, 2 of which you can access for free  
<http://advances.sciencemag.org/content/4/1/eaao5235#BIBL>

### PERMISSIONS

<http://www.sciencemag.org/help/reprints-and-permissions>

Use of this article is subject to the [Terms of Service](#)

---

*Science Advances* (ISSN 2375-2548) is published by the American Association for the Advancement of Science, 1200 New York Avenue NW, Washington, DC 20005. 2017 © The Authors, some rights reserved; exclusive licensee American Association for the Advancement of Science. No claim to original U.S. Government Works. The title *Science Advances* is a registered trademark of AAAS.